

# Simulations of grain-boundary structure

P. R. HOWELL, I. T. KILVINGTON, A. WILLOUGHBY, B. RALPH

*Department of Metallurgy and Materials Science, University of Cambridge, UK*

This paper reports some recent investigations of grain boundaries using a bubble model and a magnetic ball model. The findings are in broad agreement with current structural theories, although certain of the configurations observed are more complex than those envisaged by the purely geometrical approaches of many of the theoretical models of grain boundary structure.

## 1. Introduction

Over the past few years, renewed interest has been shown in the structure and properties of grain boundaries [1-5]. The two major investigative techniques employed in the study of grain-boundary structure have been transmission electron microscopy [6-10], and field-ion microscopy [11-15]. In both cases, the resolution is sufficient to enable the quantitative analysis of many of the features which characterize the various theoretical models; however, it is insufficient for those features where the resolution necessary for analysis is  $\approx 0.1$  nm. The only method, which is currently available, for the analysis of the fine scale structure of grain boundaries is that of "atomic modelling", and

this paper will describe some results pertaining to the various theoretical models and their interrelation from studies of a bubble model [16] and a ball model [17]. Fig. 1a and b show the general feature of the two simulations. In both cases, the rafts are "polycrystalline", the "grain boundaries" being indicated by the arrows. Fig. 1a is a bubble raft, the "atoms" being in contact both in grain, and at the grain boundaries. Fig. 1b is a ball model, and in this case, the balls are not in contact due to the repulsive forces between the individual ballbearings (created by an alternating magnetic field as per [17]). Due to the limited dimensions of the ball raft, the shape of the annulus needs to be considered when attempting to quantify results as per Section 2.1 since

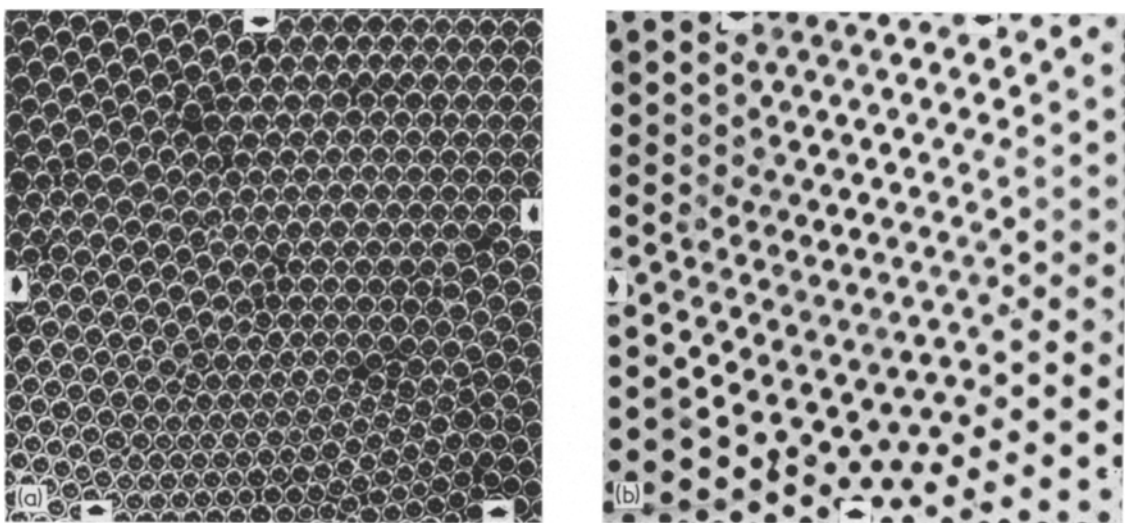


Figure 1 Examples of polycrystalline arrays as observed in this investigation. (a) A polycrystalline bubble raft. The boundaries are indicated by the arrows. Other lattice defects (such as point defects and dislocations) are also present in this raft. (b) A ball model raft. The boundaries are indicated by the arrows.

distortions in the close packed nature of the balls occur close to the annulus, and certain preferred misorientations can be produced.

## 2. Results

### 2.1. Axis/angle pair determination

The measurement of axis/angle pairs from the models is a simple process, the axis always being  $\langle 111 \rangle$  (referred to an fcc structure), and the maximum possible angle of misorientation being  $30^\circ$  (due to the six-fold symmetry of the two dimensional layer). Hence, primary twin configurations cannot be investigated using these simulations. Figs. 2 and 3 show histograms of the observed angles of misorientation for the two methods employed, Fig. 2 being collated from the

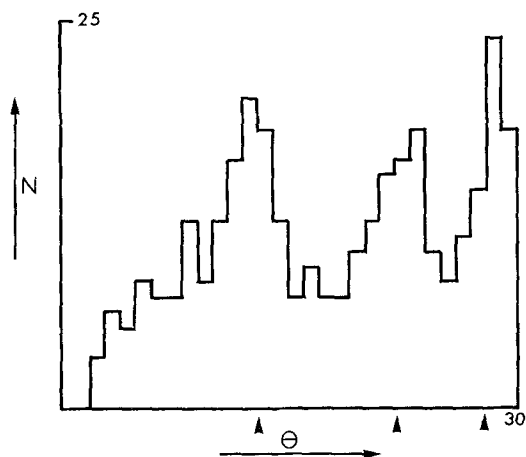


Figure 2 A histogram of the number of boundaries of a particular misorientation ( $N$ ) plotted as a function of misorientation ( $\theta$ ), collated from the bubble model. Strong peaking is observed at angles corresponding to high density coincidence site structures.

bubble model, and Fig. 3 from the ball model. Fig. 2 shows peaks in the distributions at  $\theta \approx 13^\circ$ ,  $22^\circ$  and  $28^\circ$  corresponding to the three most densely packed coincidence site structures of  $\Sigma = 19$  at  $13^\circ 10'$ ,  $\Sigma = 7$  at  $21^\circ 50'$ , and  $\Sigma = 13$  at  $27^\circ 46'$  misorientation respectively.

The histograms shown in Fig. 3 do not show such well-defined peaks and this, in part, is explained by the annular shape. The data used to construct Fig. 3a come from rafts where the restraining annulus was circular, and the observed distribution is fairly random over the whole angular range. The data used for Fig. 3b come from rafts with an hexagonal annulus and many low-angle boundaries are observed. The histogram shown in Fig. 3c relates to data

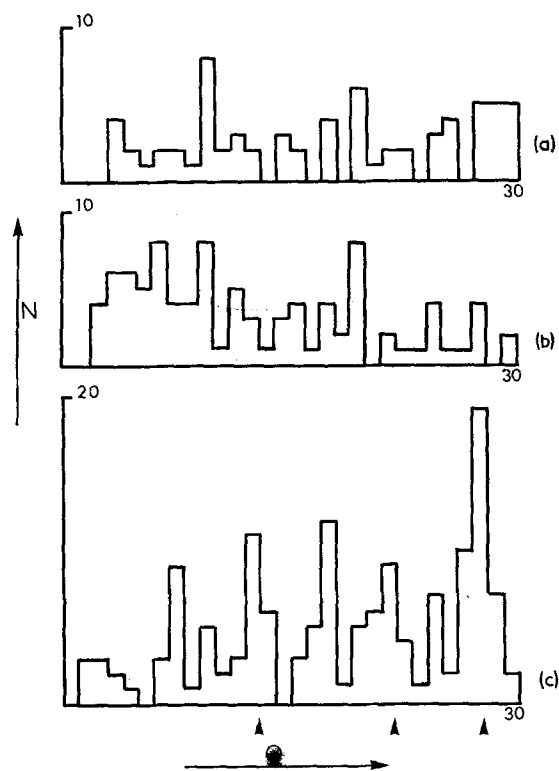


Figure 3 As for Fig. 2, but collated from the ball model, giving angular distributions for (a) the balls being constrained to lie within a round annulus; (b) the balls being constrained to lie within a hexagonal annulus; (c) the balls being constrained to lie within a square annulus. (See text.)

collated from rafts with a square annulus, and a strong peak is observed at  $\theta \approx 30^\circ$ .

A variety of other factors influence the accuracy in determining the angle of misorientation, one being the finite size of the two dimensional raft. We can estimate the minimum angle of misorientation that can be observed in these simulations.

In the absence of other crystal defects, a low-angle grain boundary may be detected if the dislocation spacing in the relaxed boundary is about one half the raft size (i.e. at least two dislocations are seen).

Thus:

$$\theta_{\min} \approx \frac{b}{h}$$

where  $b$  is the Burgers vector, and  $h$  is one half the raft size. Using typical values for  $h$  as used in these experiments,  $\theta_{\min}$  is given by 1 to  $2^\circ$ . However, in practice  $\theta_{\min}$  is somewhat higher due to the polycrystalline nature of the rafts, and this

explains the “cut-off” observed in the histograms of Figs. 2 and 3.

Other factors which have been seen to affect the measurement of angular misorientations are the presence of matrix dislocations in the vicinity of the boundary, and grain-boundary dislocations of the Van der Merwe type [5]. The configuration depicted in Fig. 4 illustrates this

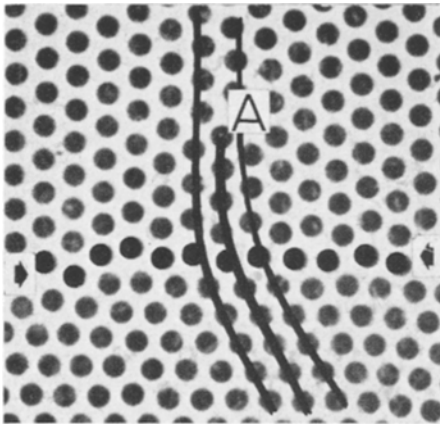


Figure 4 A grain boundary (arrowed) as observed in the ball model. A matrix dislocation is situated close to the boundary (at A), and considerable distortion of the “atom” rows in the vicinity of the dislocation is apparent.

effect, the distortion of the structure rows in the vicinity of the dislocation being considerable. Hence, measured values of the angular misorientation can vary along the grain-boundary traces by up to  $3^\circ$ .

## 2.2. Observations of grain-boundary dislocations

As discussed in [5], general grain boundaries may be thought of as being comprised of a variety of dislocation arrays. These arrays can be classed as either coincidence site structure dislocations [6-8] or Van der Merwe dislocations [5]. For the special case of low-angle grain boundaries, both classes have equivalent Burgers vectors (being equivalent to a structural vector), whereas for the more general high-angle grain boundaries, the former are characterized by partials in a coincidence site structure, while the latter are independent of the coincidence site structure. This section will discuss the observation of such defects in relation to the observed fine scale structure of the boundaries analysed.

As the rafts are two dimensional with  $\langle 111 \rangle$  the axis of misorientation, the only Van der Merwe dislocations that can be observed are

those which are created by asymmetry in the rotation about  $\langle 111 \rangle$ . Example of Van der Merwe type dislocations are given in Fig. 5a and b (being from a bubble model and ball model, respectively). The agreement between observed and calculated dislocation spacings was, in all cases, to within a few percent. In obtaining the calculated defect spacing, it was necessary to construct an “average grain-boundary trace” [18] since the boundaries observed normally exhibited a highly complex topographical structure [13].

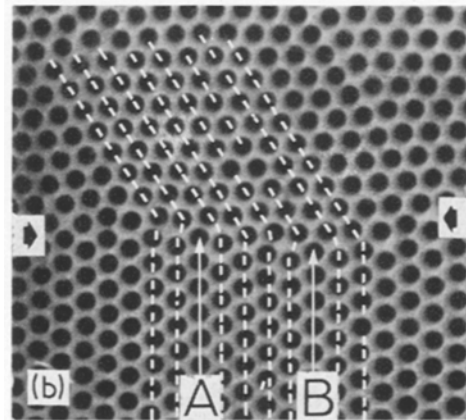
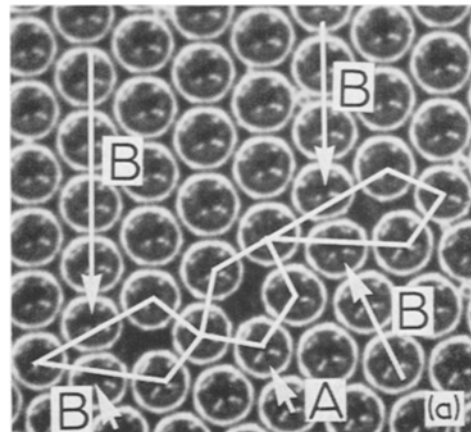


Figure 5 Examples of grain boundary dislocations of the Van der Merwe type. (a) A Van der Merwe dislocation (at A) as observed in the bubble model. The morphology of the associated structure unit is similar to that simulated by computational methods [20]. The considerable distortion of the “atoms” defining the terminations of the structure rows (B) is due to the non-equilibrium spacing of the atoms in contact across the boundary. (b) Van der Merwe dislocations as observed in a grain boundary (arrowed) in the ball model (at A and B). In this case, it is impossible to define a boundary structure unit configuration (compare with Fig. 5a).

An interesting point which will receive further attention in Section 2.3 is the shape of the observed boundary structure unit in the vicinity of the terminating half plane in Fig. 5a.

Owing to the complex nature of the majority of boundaries studied, coincidence site structure dislocations (other than those characteristic of a  $\Sigma = 1$  configuration) were rarely seen, although dislocations of the type described in [16] were occasionally observed.

### 2.3. Observations of grain-boundary structure units

Bishop and Chalmers [2] have proposed that a coincidence site boundary can be described in terms of a regularly repeating structure unit. For general boundaries, structural units from the nearest coincidence site orientations may be used to describe the boundary; this description being equivalent to one using dislocations. This section will cite some examples of observed structure unit configurations observed in a variety of boundaries.

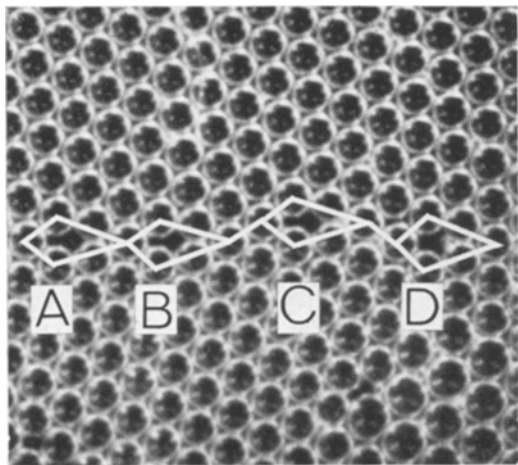


Figure 6 Structural units comprising a  $\Sigma = 7$  grain boundary. The structural unit C is seen to be on an adjacent coincidence-site structure plane to A, B and D.

Fig. 6 shows some general features of the structure units observed in this study. In this figure the structure units are characteristic of a  $\Sigma = 7$  coincidence-site structure ( $\theta \simeq 22^\circ$ ), and an interesting point to note is the fact that these structural units are seen to occur on two adjacent structural rows in the coincidence site structure which is not to be expected from the purely geometrical approach [2].

Other observations using both the bubble

model and the ball model showed the effect of introducing small translations along the boundary trace (as per Fig. 1.36 of Gleiter and Chalmers [19]) and "misfit segments" due to coincidence site structure dislocations (as per Fig. 1.8 of Gleiter and Chalmers [19]).

Fig. 5a shows the effect of introducing asymmetry in the rotation about  $\langle 111 \rangle$ , the "structure unit" in the vicinity of the extra half plane being similar to that proposed by Hasson and co-workers [20] (compare with Fig. 11 of their paper).

In general, the structures observed in near coincidence grain boundaries were more complex than those envisaged by Bishop and Chalmers [2], but were very similar to those predicted by the recent computational models [20, 21].

### 2.4. Grain-boundary segregation

Grain-boundary segregation may be studied using both the models so far described. In the present investigation, segregation of "solute atoms" has been observed to a variety of boundaries, certain specific sites being preferentially decorated with impurity.

In many cases, solute atoms were seen at the termination of the extra half planes of Van der Merwe dislocations, this site being occupied since the presence of the solute atom minimizes the compressional stresses due to this particular type of grain-boundary defect. Fig. 7 illustrates the other type of condensation profile encountered, the solute atom being localized inside

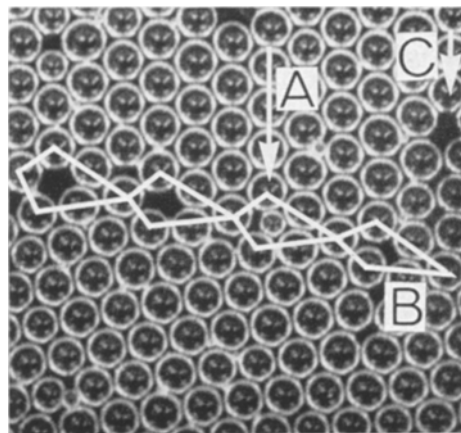


Figure 7 A solute atom which is associated with a grain boundary structure unit (at A). The distortion of the structural unit B is due to the presence of the matrix dislocation C.

the structure units comprising the boundary. Again, this result is not surprising since the structure unit as proposed must comprise alternate areas of tension and compression (even for a coincidence site structure boundary) due to non-equilibrium spacing of the atoms defining the boundary structure units.

### 2.5. Grain-boundary topography

As has been already mentioned, the grain-boundary topography was, in general, highly complex (e.g. Fig. 1a and b) unless great care was taken during the formation of the two dimensional rafts. This complex topographical structure normally precludes the possibility of analysing the coincidence-site structure dislocations as per Schober and Balluffi [6-8].

## 3. Discussion

This section will briefly discuss the results obtained during the investigation and their relevance to current structural theories and will discuss the relative merits and drawbacks of the techniques employed.

### 3.1. Structural studies

The observation of Van der Merwe dislocations in the majority of grain boundaries analysed indicates the importance of this class of defect, and is completely at variance with the results obtained by Longinov [22] and his subsequent structural theory which he based on a concept of "complete conjugation". In this model, the term complete conjugation implies that the flux of planes terminating on the boundary is equal in the two crystals. However, this can only be true if the boundary is in a symmetrical tilt orientation, or when the length of boundary analysed is less than the dislocation spacing (equivalent to the coherency criterion for interphase interfaces [18, 23].

The observations of structure units in grain boundaries during this study has shown them to be far more complex than those envisaged by a simple geometrical approach and the existence of structure units on adjacent coincidence site structure planes implies that a stacking fault has been introduced into the basic coincidence site structure. It has been shown that asymmetric boundaries produce configurations similar to those predicted [20], the "odd structure units" characterizing the extra half plane of the Van der Merwe dislocations.

It would appear, from the present studies, that

certain sites in the boundary are preferential sinks for solute, and hence one might expect, in real situations, to produce some form of "solute wavelength" in the boundary, that wavelength being characteristic of the structure units comprising the boundary. Since a study of this kind requires atomic resolution, the only technique available is field-ion microscopy, and thus far, no such evidence of a solute wavelength, has been forthcoming [24-26].

### 3.2. The methods employed

Both techniques employed in this study are useful for investigating a variety of grain-boundary phenomena, although, for any one particular application, one technique may be preferable to the other. The problem of annular shape in the ball model has already been mentioned, although this problem can be minimized by increasing the size of the raft such that "edge effects" become of relatively minor importance. Both models can be used to simulate the dynamic properties of grain boundaries, but these studies have been considered elsewhere [27]. In analysing solute/grain-boundary interactions, the bubble model has proved the more successful thus far; problems being encountered in using different ball sizes due to the fact that the "solute atoms" (in this case being balls of smaller diameter) tend to attach themselves to the larger solvent atoms". At present, work is being directed at using balls with dissimilar permeabilities but with equal dimensions.

The major drawback of both techniques is their two-dimensional nature. Hence only tilt grain boundaries may be analysed. In an attempt to investigate the structure of twist grain boundaries, two ball rafts were stacked on top of each other in the magnetic field; the resulting dislocation arrays being analysed in terms of the Moiré fringes so produced. The main problem encountered in this study was the difficulty experienced in producing single crystal rafts, the Moiré patterns being highly complex and difficult to analyse.

The other boundary models not specifically mentioned here are those of computer simulation [20, 21] and Moiré fringe modelling [13, 10, 24]. The former has the advantage, that the interatomic potentials can be chosen at will, although it is interesting to note the similarity between the examples cited here and the simulations of the various computer models. Moiré fringe modelling has an advantage in its capa-

bility for analysing both tilt and twist grain boundaries, and the Van der Merwe dislocations produced by rotation other than that about the primary axis of rotation [10, 24].

### Acknowledgements

The authors are grateful to Professor R. W. K. Honeycombe for providing laboratory facilities. The research was performed as part of a series of undergraduate projects and I.T.K. and A.W. are grateful to their Local Authorities for maintenance awards. P.R.H. wishes to acknowledge post doctoral support from the U.K.A.E.A. Mr D. Cowan and Mr J. Reich provided expert technical assistance which the authors gratefully acknowledge.

### References

1. D. G. BRANDON, B. RALPH, S. RANGANATHAN and M. WALD, *Acta Met.* **12** (1964) 813.
2. G. H. BISHOP and B. CHALMERS, *Scripta Met.* **2** (1968) 133.
3. W. BOLLMAN, "Crystal Defects and Crystalline Interfaces" (Springer-Verlag, Berlin, 1970).
4. H. GLEITER, *Phys. Stat. Sol. (b)* **45** (1971) 9.
5. B. RALPH, P. R. HOWELL and T. F. PAGE, *ibid (b)* **55** (1973) 641.
6. T. SCHÖBER and R. W. BALLUFFI, *Phil. Mag.* **20** (1969) 51.
7. *Idem, ibid* **21** (1970) 109.
8. *Idem, Phys. Stat. Sol. (b)* **44** (1971) 103.
9. J. LEVY and C. GOUX, *Mem. Sci. Rev. Met.* **44** (1967) 664.
10. P. H. PUMPHREY, Ph.D. Thesis University of Cambridge (1970).
11. B. LOBERG and H. NORDEN, *Arkiv fur Fysik* **39** (1969) 383.
12. *Idem, ibid* **40** (1970) 413.
13. P. R. HOWELL, T. F. PAGE and B. RALPH, in "Grain Boundary Structure", review course (Institution of Metallurgists, London, 1972).
14. *Idem, Phil. Mag.* **25** (1972) 879.
15. T. F. PAGE, P. R. HOWELL and B. RALPH, *J. Appl. Phys.* **44** (1973) 902.
16. Y. ISHIDA, *J. Mater. Sci.* **7** (1972) 72.
17. M. F. LONGINOV, *Fitz Metal Metalloved* **27** (1969) 104.
18. A. HILDON, P. R. HOWELL, T. F. PAGE and B. RALPH, *J. Microsc.* **99** (1973) 29.
19. H. GLEITER and B. CHALMERS, *Prog. Mat. Sci.* **16** (1972) 1.
20. G. HASSON, M. BISCONDI, P. LAGARDE, J. LEVY and C. GOUX, in "The Nature and Behaviour of Grain Boundaries", (edited by Hsun Hu) (Plenum Press, New York, 1972) p. 3.
21. M. WEINS, B. CHALMERS, H. GLEITER and M. F. ASHBY, *Scripta Met.* **3** (1969) 60.
22. M. F. LONGINOV, *Fitz Metal Metalloved* **27** (1969) 95.
23. A. HILDON, P. R. HOWELL, A. YOULE, R. J. TAUNT, T. F. PAGE and B. RALPH, *J. Microsc.* **99** (1973) 41.
24. P. R. HOWELL, Ph.D. Thesis Cambridge University (1972).
25. P. R. HOWELL, D. FLEET, T. F. PAGE and B. RALPH, *Proceedings of the Third International Conference on the Strength of Materials* **1** (1973) 149.
26. D. A. SMITH and G. D. W. SMITH, *ibid* **1** (1973) 145.
27. M. F. LONGINOV and V. F. NOSACH, *Phys. Met. Metallogr.* **31** (1971) 116.

Received 13 May and accepted 22 May 1974.